A MENAGERIE OF STELLAR FLARES

K.W. Smith[1,2], M. Audard[1], and M. Güdel[1]

[1]Paul Scherrer Institut, Würenlingen and Villigen, CH-5232 Villigen PSI, Switzerland
[2]Institute of Astronomy, ETH Zürich, CH-8092, Switzerland

Abstract

We show simultaneous X-ray and radio lightcurves obtained with XMM EPIC cameras and the VLA, for a number of active stars. A number of flares were detected, and the relationship between the X-ray and radio data in the various cases is discussed. Correlations between the timing of X-ray and radio events can be used to constrain the relationship between the fast gyrosynchrotron-emitting electrons and the heating they cause in the chromosphere and corona.

1. Introduction

Standard models of Solar flares envisage the key process to be acceleration of electrons and ions by magnetic reconnection. The energy in the electron (or ion) beam then gives rise to the flare emission in one way or another. Three emission mechanisms can be identified. First, gyrosynchrotron emission from the magnetically confined beam. This accounts for a small fraction of the energy. Second, hard X-ray emission produced as the beam impacts the chromosphere. Third, soft X-ray emission from evaporating chromospheric material heated to around 10^7K. There is therefore a physical relationship between the radio gyrosynchrotron emission and the X-ray emission. This can manifest itself in various observable effects, both in the average and in individual events (e.g. Benz & Güdel, 1994, A&A 285, 621).

An example of such a relationship is the Neupert effect. This arises because the gyrosynchrotron emission is proportional to the instantaneous number of fast particles, whilst the slowly variable soft X-ray emission is roughly proportional to the accumulated total energy. Thus;

$$L_R(t) \propto \frac{d}{dt} L_X(t) \quad (1)$$

Significant deviations from this scenario are also observed (e.g. heating starting before hard X-rays, or an absence of one emission type). Detailed analyses of the clearest examples of the Neupert effect are discussed in other papers in these Proceedings elsewhere ('An XMM-Newton study of Proxima Centauri', Guedel et al, and 'The Neupert effect in σ Geminorum', Smith et al). In this paper we present a collection of time series observations for three other active stars, all of which are M dwarfs. In each case, we have combined VLA radio observations with simultaneous XMM EPIC observations, to detect any telltale relations between the gyrosynchrotron radio and soft X-ray emission.

2. AU Mic

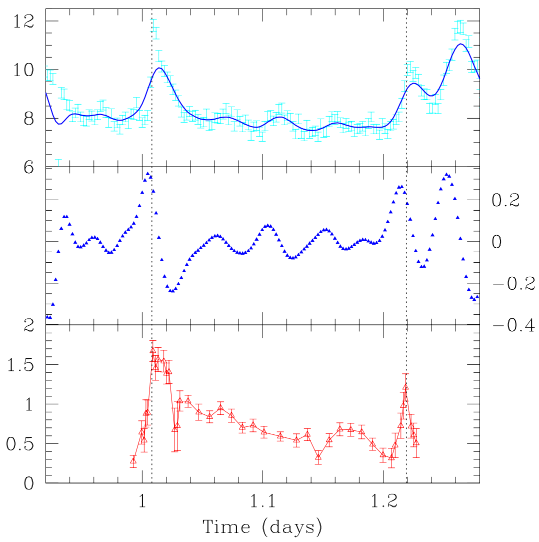

Figure 1. X-ray flux (top), derivative of X-ray flux (middle) and radio flux (bottom) for AU Mic.

The XMM pn and VLA 5GHz lightcurves are shown in Figure 1. The top panel shows the XMM pn lightcurve, and a smoothed version of this made by convolving with a Gaussian of σ equivalent to 6 data points (solid blue line). The middle panel shows an estimate of the time derivative of the X-ray lightcurve, made by averaging the gradient of the smoothed curve over three successive points. The bottom panel is a radio lightcurve made by mapping the source at each scan and fitting with a Gaussian. The main advantages of this technique are optimum time sampling, and that it provides an estimate of the error which takes account of the local background. Our X-ray and radio lightcurves both show two episodes of flaring behaviour, with a more-or-less quiescent spell in between. The radio and X-ray activity is approximately simultaneous (see vertical lines), suggesting that we are seeing a

Proc. Symposium *'New Visions of the X-ray Universe in the XMM-Newton and Chandra Era'* 26–30 November 2001, ESTEC, The Netherlands
ESA SP-488, August 2002 eds. F. Jansen & TBD

Neupert effect. Although the radio lightcurve correlates quite strongly with the X-ray derivative, it shows a lag of about 10 minutes in each case.

3. AD Leo

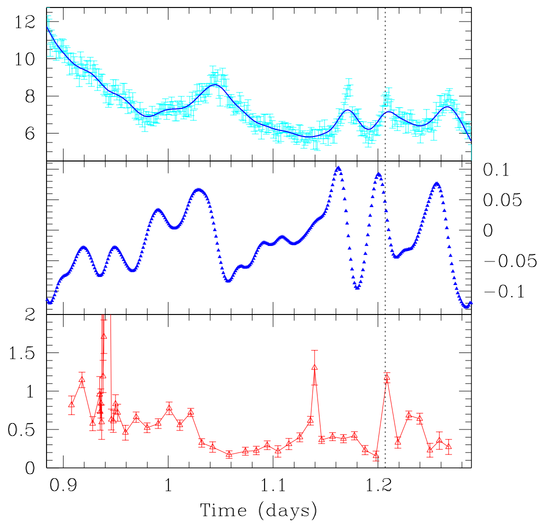

Figure 2. Top panel: EPIC lightcurve, points and smoothed curve. Middle panel: Time derivative of the X-ray lightcurve. Bottom panel: Radio lightcurve at 5GHz.

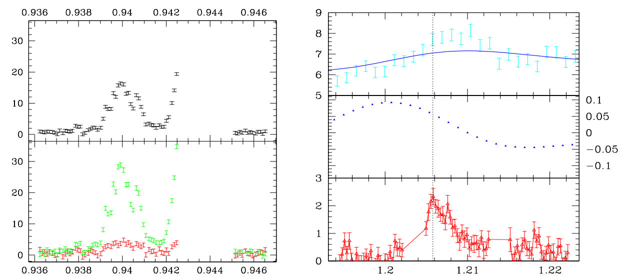

Figure 3. Left: Closeup of the radio lightcurve for the first event. The top panel shows the total radio flux. The gap is the break between scans, during which time the phase calibrator was observed. The lower panel shows separately the left (green) and right hand (red) circularly polarized flux. Right: Closeup of the event at 1.2 days, showing the relative timing of the X-ray flux, derivative of X-ray flux and radio flux.

The X-ray lightcurve of AD Leo (see Figure 2 shows a decay from a large earlier event. There is evidence of this too in the radio lightcurve. A very large, sharp event is seen at 5GHz in the early part of the observation. There is no apparent corresponding soft X-ray activity at this point. A time-symmetric X-ray brightening occurs about two hours later, but this is probably unrelated. Examination of the separate Stokes LL and RR components reveals that the early radio flare is strongly Left hand circularly polarized, suggesting that this may be a coherent emission process requiring fewer accelerated particles and hence leading to negligable chromospheric heating (Figure 3, left hand panel). There are three further X-ray flares and two further radio events towards the end of the observation. The first radio event preceeds the first X-ray event by approximately 45 minutes and these are probably not related. The second radio flare is approximately simultaneous with the second X-ray flare (Figure 3, right hand panel).

4. UV Ceti

For this star, we obtained radio data at both 5 and 8.3 GHz. These are shown as separate red (8.3GHz) and green (5GHz) curves in the lower panel of Figure 4. UV Ceti showed little X-ray activity during our observations (top panel). A small flarelike event can be seen just short of 0.7 days. This is accompanied by a simultaneous radio flare (bottom panel). The spectrum is falling, indicating synchrotron emission, and the preferential brightening of the low frequency flux shows that the spectrum is steepening during the flare. The 5GHz peak occurs during the decay phase of the X-ray flare. This situation cannot be explained by a Neupert-like scenario and may indicate changing absorption of the radio flux during the event.

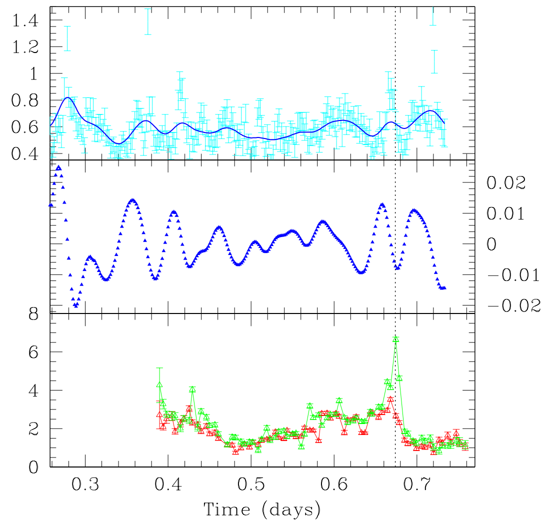

Figure 4. X-ray flux (top), derivative of X-ray flux (middle) and radio flux (bottom) for UV Ceti.

References

Benz A.O., & Güdel M., 1994, A&A 285, 621

Güdel M., Smith K.W., Audard, M. Skinner, S.L. & Drake J., 2002, this volume

Smith K.W., Güdel M., Audard M, Behar E. & Mewe R. 2002, this volume.